Supporting Information

Hybrid molecule-nanocrystal photon upconversion across the visible and near-infrared

Zhiyuan Huang, Xin Li, Melika Mahboub, Kerry M. Hanson, Valerie M. Nichols, Hoang Le, Ming L. Tang*, Christopher J. Bardeen*

Department of Chemistry
University of California, Riverside
Riverside CA 92521

*e-mail: mltang@ucr.edu
*e-mail: christopher.bardeen@ucr.edu

1. Sample preparation and characterization

A) Materials

Chemical reagents were purchased from Aldrich Chemical Co, Strem, TCI America, or Alfa Aesar and were used as received. Dry and degassed acetone, toluene were obtained from JC Meyer's solvent purification system. 9,10-diphenylanthracene (DPA), 2-anthracenecarboxylic acid (2-ACA), 1-anthracenecarboxylic acid (1-ACA), and 9-anthracenecarboxylic acid (9-ACA) were obtained from TCI AMERICA, rubrene (RUB) was obtained from Acros Organics, and 9-anthracenepropionic acid was obtained from Molecular Probes.   All molecules were used as received.

B) Instrumentation

Absorption spectra were recorded on a Jasco-V670 UV-Vis absorption spectrophotometer. Ensemble fluorescence spectra were recorded on a HORIBA FluoroMax-3 fluorometer. Upconversion fluorescence spectra were recorded on an Ocean Optics Inc. JAZ spectrometer.   Fluorescence signals for the power-dependence and quantum yield measurements were acquired using a Hamamatsu H5783 photomultiplier tube equipped with interference and edge filters to isolate the RUB and DPA emission wavelengths.   Lasers used: 532 nm light was obtained from a Coherent Sapphire diode laser, with an output power of 10 mW.   800 nm laser light was obtained from a Kapteyn-Murnane Labs Ti:Sapphire laser pumped by a Spectra Physics Millenia laser.   The laser was operated in cw mode.   980 nm laser light was obtained from a Amonics ALS-980-MM-1-SA fiber-coupled diode laser.   Laser powers were measured using an Ophir Vega power meter with 3A and PD300 low power detector heads.

Transmission electron microscopy was performed on a Tecnai12 TEM. NMR spectra were recorded on a Varian Inova-400MHz NMR spectrometer at room temperature. The ^{1}H Chemical shifts (δ) are reported in parts per million with residual solvent ($CHCl_3$) peak as an internal standard.

C) Nanoparticle synthesis

C.1) Synthesis of CdSe nanocrystals

CdSe nanocrystals (NCs) were synthesized and purified by the procedure published by Carbone et al.[1] Trioctylphosphine oxide (TOPO) (3.0g), octadecylphosphonic acid (ODPA) (0.280g) and CdO (0.060g) were mixed in a 25mL three neck flask, heated to ca. 150°C and exposed to vacuum for 1 hour. Then, under Ar (g), the solution was heated to above 300°C to dissolve the CdO until it formed a clear light yellow solution. At this point, 1.5 g of trioctylphosphine (TOP) was injected and the temperature was allowed to recover to the value required for the injection of the Se:TOP solution (0.058g Se + 0.360g TOP) to create a NC with a specific diameter. For example, for the synthesis of 3.28 nm diameter CdSe, the injection temperature was 375 °C.   Immediately after injection, the reaction flask was cooled down quickly with compressed air. After the synthesis, as-prepared CdSe NCs were transferred to the glove box and cleaned with methanol and toluene at least three times. The final pellet was dissolved in toluene and stored inside a nitrogen glove box for future use. The NC concentration and diameter was determined by measuring the absorbance at the first exciton absorption maxima and calculated according to Yu et. al[2]. The photoluminescence quantum yield of the 3.28 nm diameter particles was measured to be 0.12 using Rhodamine6G (quantum yield = 0.95) as the standard.
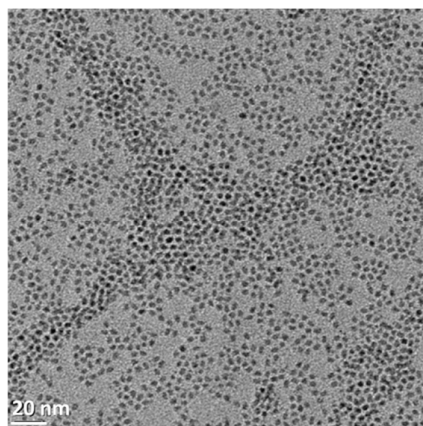
Figure S1. TEM of the 3.28 nm diameter CdSe NCs.

C.2) Synthesis of PbS nanocrystals [3]

PbO (0.45 g), oleic acid (OA, 10 mL), and 1-octadecene (ODE, 10 mL) were mixed in a 50 ml three-neck flask and heated to 110 °C under vacuum for an hour. Pb oleate is formed, indicated by the discoloration of the reaction to a clear light yellow solution. Then, the reaction flask was backfilled with Ar (g), and heated to 150 °C. At 150 °C, the sulfide precursor, containing 0.21 mL of bis(trimethylsilyl)sulfide in 10 mL of anhydrous ODE, was injected, and the temperature dropped to about 130 °C. The reaction flask was allowed to cool down to 100°C for 3 min by turning off the heater. Then the reaction flask was kept at 100 °C for 5 min. The PbS NCs were transferred to a glovebox and washed 3 times by adding 1:1 hexanes/ethanol mixture; followed by centrifuging at 7000 rpm for 5 min. The supernatant was discarded. The final pellet was dissolved in hexane and stored in the dark inside the glovebox for future use. The PbS NC size (3.1 nm diameter) was determined by measuring the energy of the first exciton peak. The concentration of the PbS NCs was determined from the absorption at 400 nm[4].
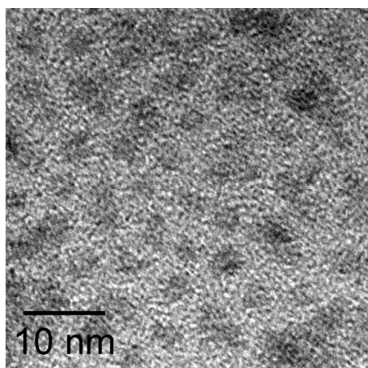

Figure S2. TEM image of the 3.10 nm diameter PbS nanoparticles.

C.3) Synthesis of PbSe nanocrystals

The same general method in Section (C.2) above was used, with the only difference being that a selenide precursor was used, i.e. 0.21 ml bis(trimethylsilyl)selenide instead of 0.21 ml bis(trimethylsilyl)sulfide. The size and concentration of PbSe nanocrystals were determined by measuring the energy of the first exciton peak and the absorption at 400 nm respectively[5].
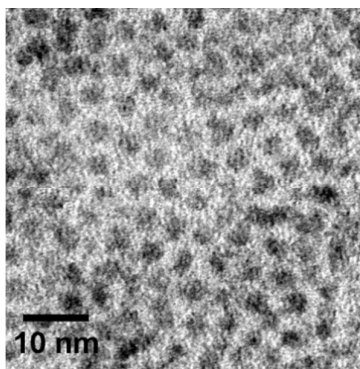
Figure S3. TEM image of 2.10 nm diameter PbSe nanoparticles.

2.   Characterization of CdSe NCs

A) CdSe + 9-anthracene carboxylic acid (9ACA) + DPA

A.1) Upconversion sample preparation using ligand exchange

0.797 ml of 3.28 nm diameter CdSe NCs in toluene (with a concentration of $2.51*10^{-5}$M) and 1.96 ml of 9-ACA in a mixture of acetonitrile:toluene = 3:11(v/v) solution(with a concentration of 0.0216 M) were mixed and stirred for 1.5 hours.   An equal volume of acetone was added. The resulting solution was centrifuged at 7830 rpm for 10 min.   The resulting pellet was redispersed in 0.98 ml toluene, followed by adding 20 μL of a 0.05M DPA toluene solution. The entire procedure was performed in a nitrogen glovebox. Note that the solubility of 9-ACA reaches a limit of 0.0216M in 3:11(v/v) acetonitrile: toluene. Upconversion samples were prepared in a N_2 glovebox with air-free cuvettes sealed with parafilm.

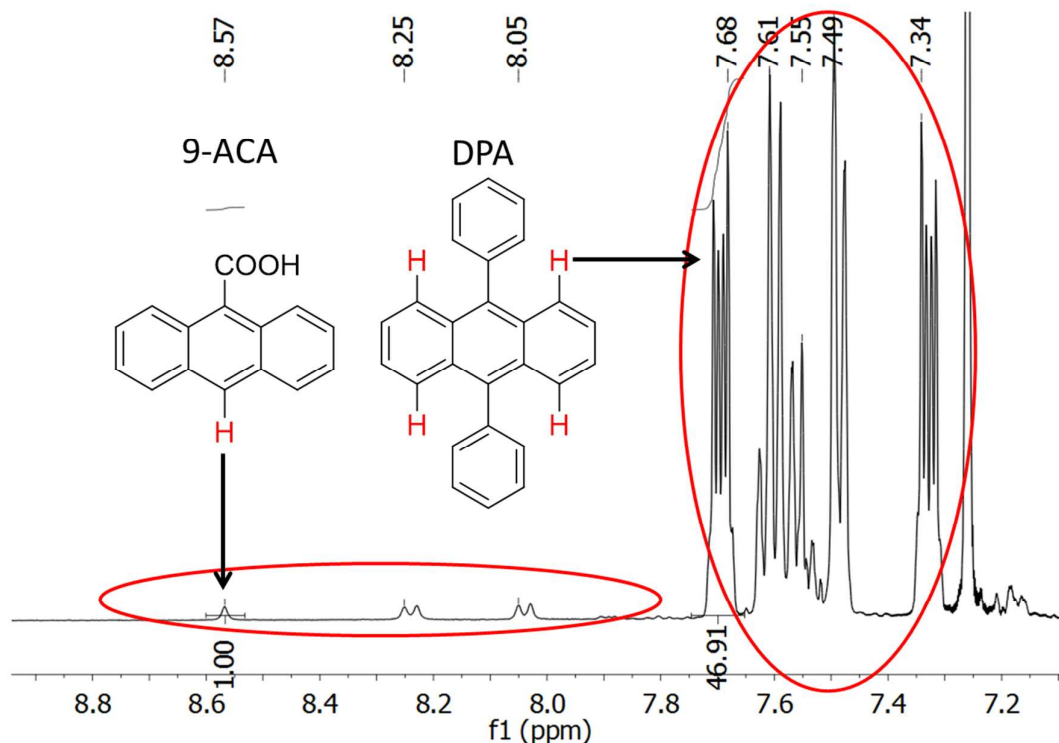**A.2) Estimation of surface coverage of CdSe by 9-ACA by NMR**

Figure S4. The NMR spectrum of the aromatic region of the sample with 0.015M of 9-ACA in the ligand exchange solution that had the highest upconversion signal from DPA. Approximately 13 transmitter 9-ACA ligands are bound per CdSe NC. See text below for details.

The NMR spectrum of the sample with the highest concentration of 9-ACA (0.015M) is shown in Figure S4. The full NMR spectrum is shown in Figure S5.   To prepare this sample, the toluene was evaporated

and the entire sample dissolved in $CDCl_3$. For 9-ACA, the singlet at 7.53 ppm corresponds to the proton at the 10 position in 9-ACA, while for DPA, the multiplet at 7.35 ppm corresponds to the 4 protons at the 1,4,5 and 8 positions on the conjugated core. Comparing the area under the 9-ACA peak to those of the DPA, we find that the molar ratio of 9-ACA and DPA is 1: 47.49/4= 1: 11.87. From this, and the known DPA concentration of 1.0 mM, the concentration of 9-ACA is calculated to 84.2 μM in the solution used for upconversion. The concentration of the 3.28 nm diameter CdSe is 6.43 μM. This gives a maximum surface coverage of 13 9-ACA molecules per particle, indicating full ligand exchange has not occurred.
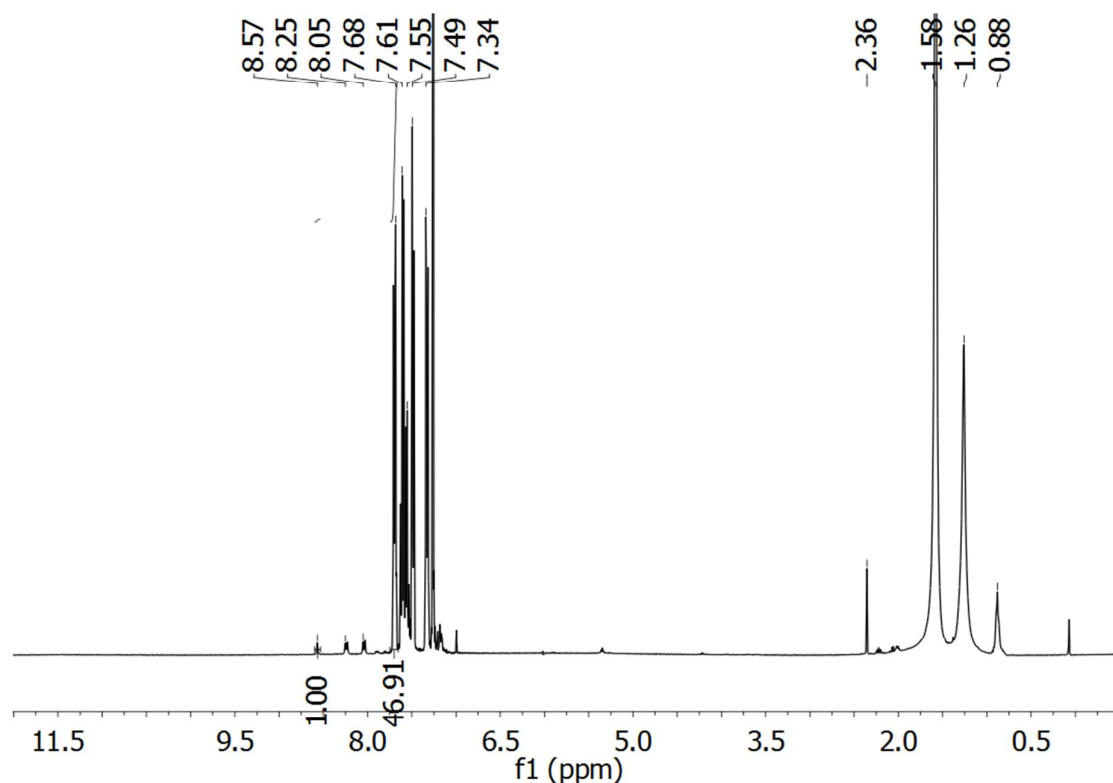

Figure S5. The full NMR spectrum of the sample in Figure S4.

A.3) Effect of concentration of CdSe

The upconversion signal was found to increase linearly with CdSe concentration over the range we studied (0.4-6 μM), as expected based on the increased absorption by the CdSe, suggesting that the upconversion yield is independent of the CdSe concentration over this range.

A.4) Effect of different anthracene ligand

Figure S6 shows the upconversion spectra taken for CdSe/DPA with the four different anthracene carboxylic acid ligands. The samples were prepared under the same conditions as described Section 2, part A.1. Because the CdSe concentration varied slightly between samples, the spectra were scaled by the different CdSe concentrations. In Figure S7, we compare the optimized CdSe/9-ACA/DPA upconversion sample to that of CdSe/ODPA/DPA. The DPA fluorescence is undetectable in the ODPA sample, and the logarithmic plot shows that the 9-ACA ligand leads to a factor of 10^3 increase in this signal above the noise.
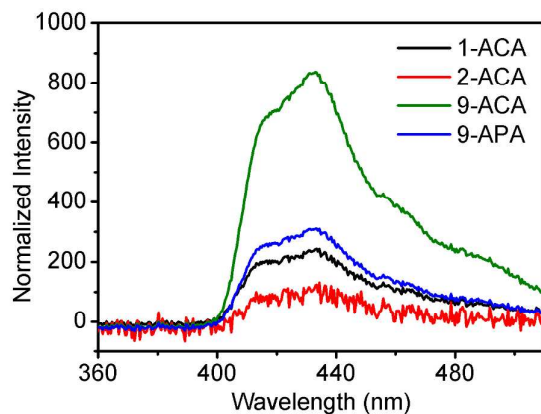
Figure S6. Upconversion photoluminescence spectra of different anthracene ligands. Samples are prepared with 1.62 mM anthracene ligands in the ligand exchange solutions. [DPA] = 1 mM. The upconversion signal is scaled by dividing the spectra by [CdSe] (in μM).
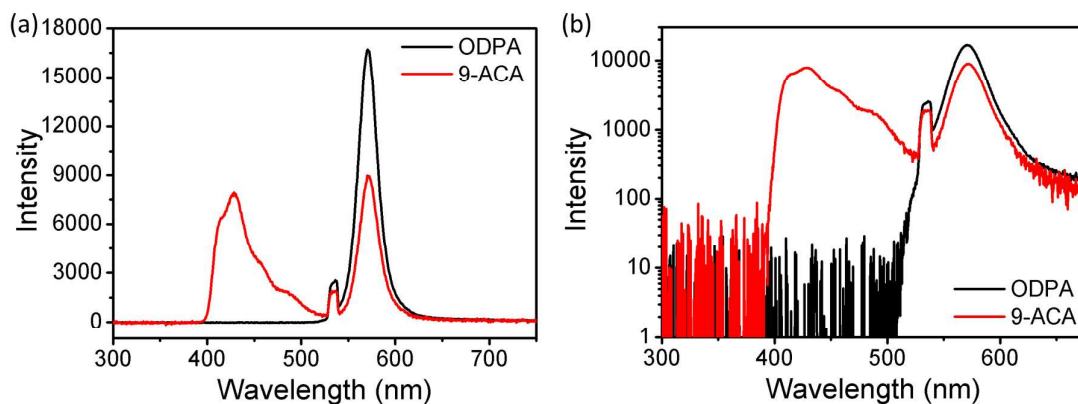

Figure S7. Upconversion photoluminescence spectra of CdSe/9-ACA/DPA and CdSe/ODPA/DPA samples plotted on (a) a linear scale and (b) a log scale. Samples are prepared as described in Section 2, part A.1, with [CdSe/9-ACA]=$3.52*10^{-6}$ M, [CdSe/ODPA]=$2.10*10^{-6}$ M, and [DPA]=1 mM.

3. Quantum yield measurements

A) Sample Preparation

CdSe+9-anthracene carboxylic acid + DPA

Ligand exchange was conducted according to the general method in Section 2 part A.1 with 54.4 ul of 2.7 nm diameter CdSe toluene solution with concentration of $8.05*10^{-5}$M, 1.96 ml of 9-ACA solution (0.0216M) in acetonitrile: toluene, 3:11(v/v), and 12 h ligand exchange time. For the quantum yield standard, Rhodamine 6G in ethanol was used (quantum yield = 0.95).

PbSe+Rubrene

41.2 μL of 2.1 nm diameter PbSe NCs in hexane solution with concentration of $1.33*10^{-3}$M, and 958.8uL rubrene in toluene solution (4.0M) was mixed.

B) Absolute Quantum Yield Calculation for CdSe

The upconversion quantum yield (Φ_{uc}) is calculated by equation S1

$$\Phi_{uc} = 2 \times \Phi_{R6G} \times \frac{n_{DPA}^2}{n_{R6G}^2} \times \frac{[Area]_{DPA}}{[Area]_{R6G}} \times \frac{1-10^{-A_{R6G}}}{1-10^{-A_{CdSe}}} \tag{S1}$$

where Φ_{R6G} is the quantum yield of R6G, n_{DPA} and n_{R6G} represent the refractive indices of the solvents for the DPA upconversion sample and R6G, which are hexane and ethanol, respectively. $[Area]_{DPA}$ and $[Area]_{R6G}$ are the integrated areas of the fluorescence peaks of DPA and R6G. A_{CdSe} and A_{R6G} stand for the absorbance of CdSe NCs and R6G at 532nm.
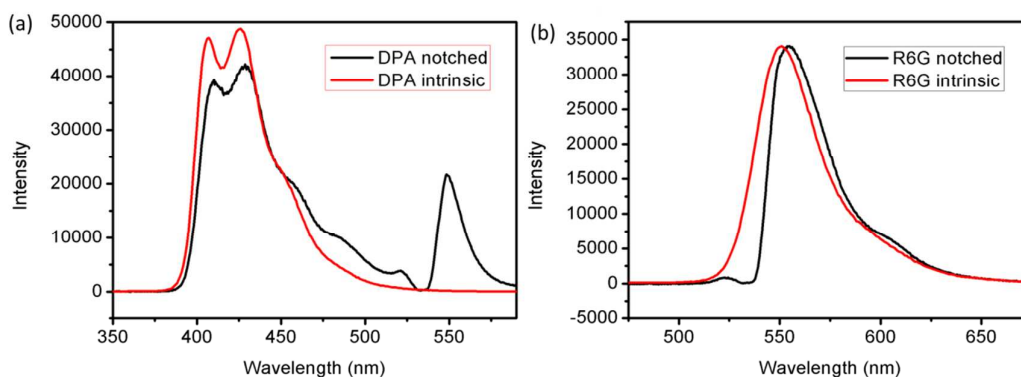

Figure S8. (a) Intrinsic (red) and detected (black) upconversion fluorescence spectra of DPA. The intrinsic fluorescence spectrum is scaled to match the upconversion spectrum at 450 nm. (b) Intrinsic (red) and detected (black) Rhodamine 6G fluorescence spectra. The intrinsic spectrum of the Rhodamine 6G standard is scaled to match the experimental spectrum at 550 nm.

The detected upconversion fluorescence spectrum of DPA and the fluorescence spectrum of the R6G standard are distorted by the presence of the 532 notch filter that is necessary to block scattered 532 nm laser light. To correct for these distortions, we scale the intrinsic fluorescence spectra so they match the detected spectra at specific wavelengths, as shown in Figure S8. We then use values Φ_{R6G} =0.95,

n_{DPA} = 1.375 and n_{R6G} = 1.360, $[Area]_{DPA}$ = 51896 (after dividing by 50 to account for integration time), $[Area]_{R6G}$ = 1555077, A_{CdSe} = 0.192 and A_{R6G} = 0.312. Plugging these values into

Equation S1 leads to a value of 0.093 for the upconversion quantum yield Φ_{uc}. Different spectral scaling methods could change this value, leading to a conservative error range of ±0.02.

C) Quantum Yield Calculation for PbSe (800 nm)

These measurements were done on samples with a PbSe nanoparticle concentration of $5.5*10^{-5}$ and [RUB] = $4*10^{-3}$ M. A demountable cell (Pike Technologies 162-1100) with a pathlength of 100 μm was used in order to make the sample optically thin and ensure a uniform beam intensity. The 800 nm beam was reflected off a dichroic mirror and focused to spot size of ~150 μm diameter. The 800 nm power was adjusted to put the upconverted fluorescence signal well into the linear regime with an intensity of 1000 W/cm^2. For the reference sample (RUB in toluene), the sample was excited at 400 nm using the frequency doubled output of a Ti:Sapphire laser. The laser beams were chopped and the output of the photomultiplier tube was detected on a lockin amplifier (SRS 810). Both the RUB and PbSe/RUB fluorescence signals were checked for linearity.

$$\Phi_{UC} = 2\Phi_{ref} \times \frac{(photons\ absorbed\ by\ reference)}{(photons\ absorbed\ by\ UC\ sample)} \times \frac{signal(UC\ sample)}{signal(reference)} \tag{S2}$$

Φ_{ref} is the quantum yield of RUB and is 0.98. The detected signals were 6.00 mV for a 18 μW of 400

nm laser power, and 2.46 mV for 192.2 mW of 800 nm laser power. Note that we use 1000x more 800 nm laser power. The absorbance of the RUB sample at 400 nm was measured to be 0.0295 using a process of serial dilution. The absorbance of the PbSe sample at 800 nm was measured to be 0.0116. The number of photons absorbed is calculated using the relation

$$photons\ absorbed\ /\ s = \frac{Laser\ Power}{hc/\lambda}\left(1 - 10^{-Abs}\right) \tag{S3}$$

h is Planck's constant, c is the speed of light, and Abs is the sample absorption. Using Equation S3 for λ=400 nm and λ=800 nm with the given powers and absorbances, we then substitute these values into

Equation S2 to obtain Φ_{UC} = $9.3*10^{-5}$. By taking possible errors in laser power, detection, and

background into account, we can find a variation of roughly $0.5*10^{-5}$, leading to our reported value Φ_{UC} = $1.0\ (\pm 0.5)*10^{-4}$.

D) Quantum Yield Estimation for PbSe (980 nm)

The 980 nm output from the fiber laser could not be focused tightly at the same location as the 800 nm beam, so we attenuated the 800 nm laser in order to put both upconversion efficiencies into the quadratic regime. We used a 1 cm cuvette that ensured that 100% of both beams was absorbed in the sample and detected the fluorescence from the front face using a photomultiplier tube. In this regime, the upconverted signal is proportional to the intensity squared multiplied by the laser spot size.

$$\frac{\Phi_{980}}{\Phi_{800}} = \frac{((800\ nm\ power)/A_{800})^2}{((980\ nm\ power)/A_{980})^2} \times \frac{A_{800}}{A_{980}} \times \frac{signal(980\ nm)}{signal(800\ nm)} \tag{S4}$$

A_{800} is the area of the 800 nm beam, and A_{980} is the area of the 980 nm beam. We measured the 800 nm power to be 7.19 mW, the 980 nm power to be 79.1 mW, the signal from the 980 nm was 25.4 mV, the signal from the 800 nm was 17.0 mV, the 800 nm beam radius was 0.074 mm, and the 980 nm beam radius was 0.54 mm. The area is proportional to the spot radius squared. Plugging all these values into

Equation S4 yielded a quantum yield ratio $\frac{\Phi_{980}}{\Phi_{800}}$ = 0.64, but we emphasize that there is quite a bit of

uncertainty in this ratio due to the nonuniform excitation intensity as the beams are absorbed in the 1 cm

cuvette, and it could be a factor of 2 higher or lower. A factor of 2 lower leads to $\frac{\Phi_{980}}{\Phi_{800}}$ = 0.32, and so

we conservatively estimate that Φ_{980} is within a factor of 3 of Φ_{800}.

4. Intensity dependence

A) Sample preparation

PbSe+rubrene

See section Section 3 part A.1. [PbSe] = $5.48*10^{-5}$, and [RUB] = 3.84 mM.

CdSe+9-ACA+DPA

The sample was prepared with the similar method in Section 2, part A, with 1.96 ml 9-ACA acetonitrile/toluene 3:11(v/v) solution.   [CdSe] = $6.05*10^{-7}$ M and [DPA]=1.00 mM.

B) Intensity dependent measurements

The low concentration of CdSe used in these measurements allowed the use of a 1 cm pathlength cuvette, since these samples were still optically thin at the 532 nm excitation wavelength.   The CdSe/DPA mixture was placed in a 1 cm cuvette and the 532 nm light was focused using a 50 cm focal length lens.   The depth of focus exceeded the detection volume.   The fluorescence was detected at a right angle to the excitation with a photomultiplier tube with filters to remove the 532 nm laser scatter and isolate the 450 nm DPA emission.   The output of the photomultiplier tube was directed into a lockin amplifier, which was synchronized to the frequency of laser modulation (200 Hz) by a mechanical chopper.   This detection system was measured to have a linear response over 3 orders of magnitude.   The laser intensity was varied by using different value neutral density filters, and the power was measured at every setting.

For the PbSe/RUB mixtures, the samples had a PbSe nanoparticle concentration of $5.5*10^{-5}$ and [RUB] = $4*10^{-3}$ M.   These samples were highly absorbing, so a demountable cell (Pike Technologies 162-1100) with a pathlength of 100 μm was used in order to make the sample optically thin and ensure a uniform beam intensity.   The 800 nm beam was reflected off a dichroic mirror and focused to spot size of ~150 μm diameter.   The laser intensity was varied by using different value neutral density filters, and the power was measured at every setting.   The fluorescence was collected using a 4 cm focal length lens behind the dichroic and focused into a photomultiplier tube.   The output of the photomultiplier tube was directed into a lockin amplifier, which was synchronized to the frequency of laser modulation (200 Hz) by a mechanical chopper.   This detection system was measured to have a linear response over 3 orders of magnitude.
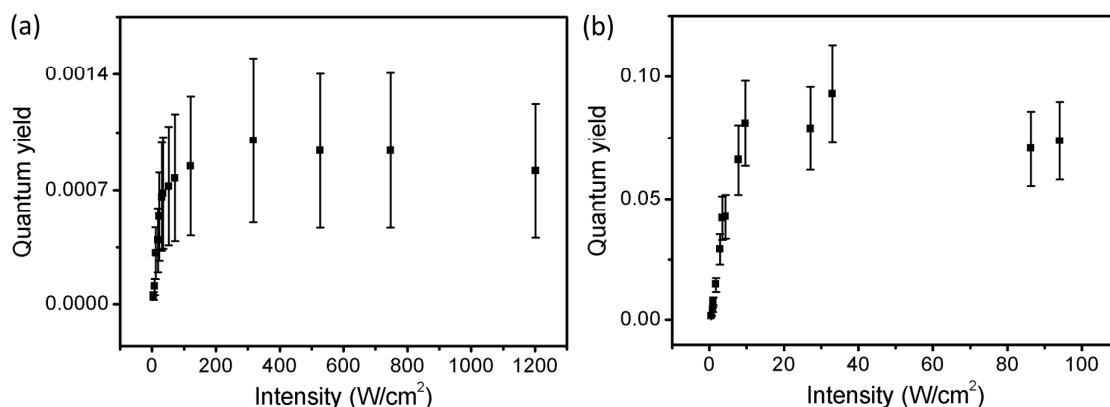
Figure S9 (a) PbSe/RUB and (b) CdSe/9-ACA/DPA upconversion quantum yields versus 532 nm and 800 nm laser intensities, respectively. This data is complements that shown in Figures 3b and 5b in the main text, showing the intensity threshold where the yield, proportional to the upconversion PL divided by absorbed laser photons, becomes independent of laser intensity.

5.   Time-resolved photoluminescence

A) Sample preparation

PbSe+rubrene
The sample was prepared as described in Section 3 part A. [PbSe] = $5.9*10^{-5}$ M, and [RUB] = 2.00 mM.

CdSe+9-ACA+DPA
The sample was prepared as described in Section 2, part A. [CdSe] = $3.5*10^{-6}$ M, and [DPA] = 1.00 mM.

B) Time-resolved measurements

A diode-pumped (Verdi, Coherent) Ti:Sapphire oscillator (Vitesse, Coherent) and Nd:YLF pumped (Evolution, Coherent) regenerative amplifier (Libra) yields 800 nm 100 fs pulses at 1 kHz (3.8 W). PbSe/RUB and RUB-only samples were excited with the 800 nm fundamental. CdSe/ODPA, CdSe/9ACA/DPA and DPA-only samples were excited at 400 nm with frequency doubled 800 nm (BBO). The sample (1 cm capped quartz cuvette) was placed such that the incident excitation beam (0.1 μW) was focused (focal length = 20 cm) on the sample.   The fluorescence was collected using front-face detection at an angle of ~10 degrees with respect to the excitation beam.   The emission was collected with a lens (f = 20 cm) and then imaged (f= 5 cm) into a Hamammatsu C4334 streak camera detector.   Residual 800 nm and 400 nm were removed with a hot-mirror and a long-wave pass 420 nm filter before the detector, respectively.   Time-resolved data for the CdSe/ODPA, CdSe/9ACA/DPA and DPA-only samples were collected using 1 ns and 100 ns sweep windows with a center collection wavelength of 570 nm. PbSe/RUB and RUB-only time-resolved data were collected at 100 ns and 500 μs sweep windows with a center collection wavelength of 600 nm.

B.1)   Characterization of delayed fluorescence from PbSe/RUB.
When 800 nm femtosecond pulses excite the PbSe/RUB sample, there are both prompt (ns) and delayed (μs) fluorescence components.   The spectra of both components are almost identical, as shown in Figure
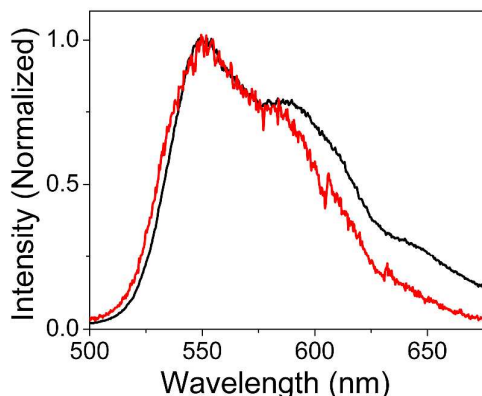
S10, and correspond to the RUB singlet emission.

Figure S10.   Comparison of early time (0-100 ns, black) and late time (0.6-390 μs, red) fluorescence from the PbSe/RUB sample after excitation with 800 nm laser pulse.   The early spectrum reflects prompt fluorescence due to nonresonant two-photon excitation of the RUB, while the delayed fluorescence is due to upconverted signal after TTA by RUB molecules sensitized by PbSe NC's.   The slightly different spectral shapes reflect additional self absorption of the prompt (two-photon) fluorescence due to the deeper penetration of the two-photon excitation mode into the sample cuvette.

B.2)   Characterization of fluorescence from CdSe/9ACA/DPA.

When the CdSe/9ACA/DPA sample is excited with 400 nm, the fluorescence is dominated by the DPA emission.   The fluorescence decays for the CdSe/9ACA/DPA sample and DPA in dilute toluene solution are identical to within the experimental error, as shown in Figure S11.
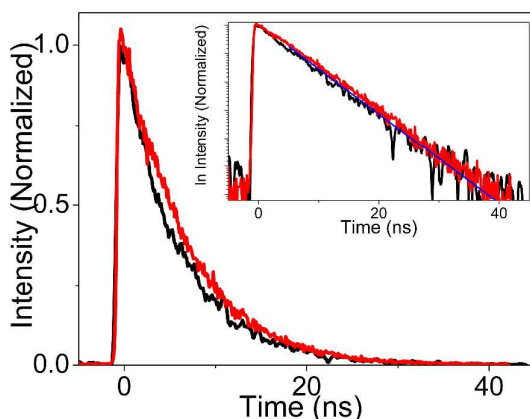

Figure S11.   Comparison of the fluorescence decays of DPA by itself (black) and the CdSe/9-ACA/DPA sample (red).   Inset: Logarithmic comparison of the decay.   Both are single exponential with a lifetime of 6.5+/-0.1 ns for the CdSe/9-ACA/DPA sample and 6.3+/-0.1 ns for the DPA sample.

B.2)   Characterization of quenching of CdSe photoluminescence by 9-ACA ligand.

Lastly, the photoluminescence decay of a CdSe/9-ACA sample was compared to that of a CdSe/ODPA sample (no DPA acceptor in either sample).   For the CdSe/9-ACA sample, the 400 nm beam excited a significant amount of free 9-ACA ligands in solution, and the narrow CdSe peak at 570 nm had to be isolated from the 9-ACA emission that stretches from 450 to 550 nm.   An example of the spectral data, along with its decomposition into 9-ACA and CdSe components, is shown in Figure S12a.   The acceleration of the CdSe component is shown in Figure S12b in the 100 ns window.
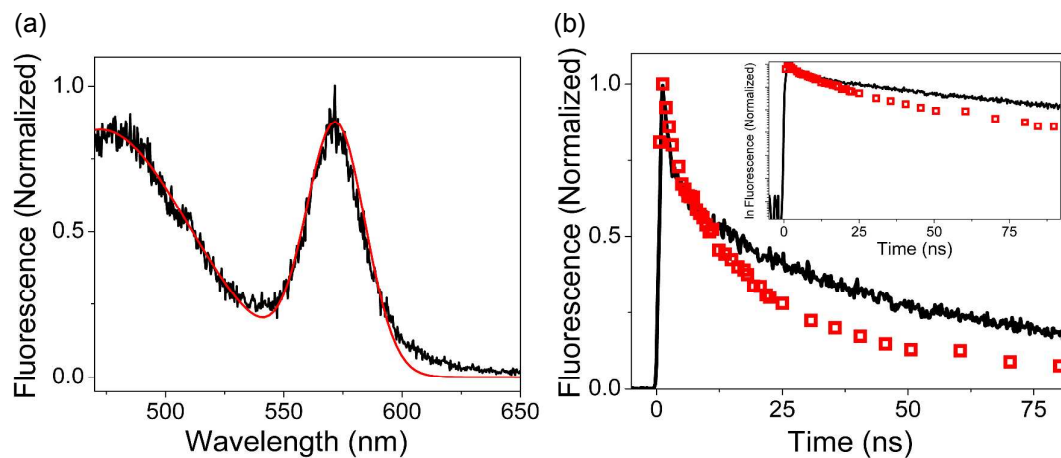
Figure S12. (a) The CdSe emission peak (centered at 570 nm) with overlapping 9-ACA fluorescence (centered at 490 nm) is fit with a dual Gaussian fit (red line) in the time window 54-75 ns. The amplitude of the Gaussian centered at 570 nm is taken to be the amplitude of the CdSe luminescence in this time window. (b) Decay of the CdSe/ODPA sample (black) and extracted CdSe component from the CdSe/9-ACA sample (red). Inset: Logarithmic comparison of the decays. Both decays are multiexponential, as typically seen for CdSe NCs, but the CdSe/9-ACA sample diverges from the CdSe/ODPA sample after 10 ns and decays more rapidly.
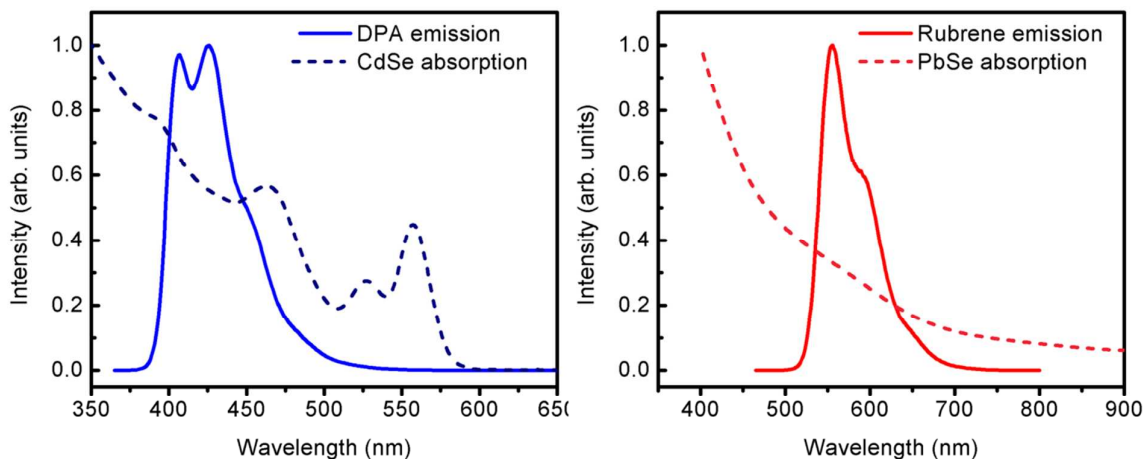
6. Förster radius calculation

Figure S13. Normalized absorption and emission for donor and acceptor pair of DPA & CdSe (left) and rubrene & PbSe (right).

The Förster radius is calculated using the standard equation below [6]:

$$R_0^6 = \frac{9000 Q_D (\ln 10) \kappa^2 J}{128 \pi^5 n^4 N_A}, \quad J = \int_0^\infty F_D(\lambda) \varepsilon_A(\lambda) \lambda^4 d\lambda$$

R_0: Förster distance

Q_D: quantum yield of donor.

κ : orientation factor, 0.667 (isotropic)

J: overlap integral.

F_D: Normalized donor emission spectrum.

$\varepsilon_A(\lambda)$: extinction coefficient of the acceptor at λ.

n: refractive index of toluene.

N_A: Avogadro constant, $6.02*10^{23}$.

	CdSe(3.2nm) & DPA	PbSe (2.1 nm) & rubrene
Q_D of donor[7]	0.97	0.98
ε_A of NC acceptor	$1.17*10^5$ (@557nm) [2]	$2.59*10^5$(@400nm) [2].
J (cm^6.mol^{-1})	$4.98*10^{-13}$	$9.29*10^{-13}$
n	1.496	1.496
R_0(Å)	57.9	64.3

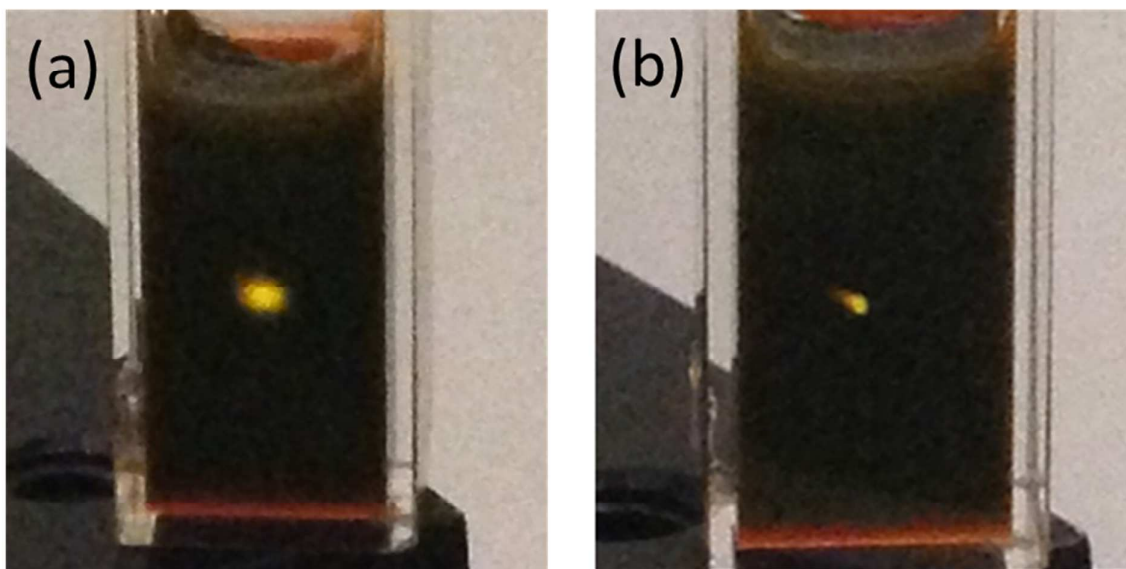# 8. Photographs of upconversion photoluminescence

Figure S14. Photographs of upconversion in a cuvette containing PbSe/RUB mixture. The yellow spot is emission from the RUB originating from (a) an unfocused cw 800 nm laser with an intensity of 300 W/cm^2. (b) a focused cw 980 nm laser with an intensity of 2000 W/cm^2. The photographs were taken with an Iphone 5 and were not modified in any way.
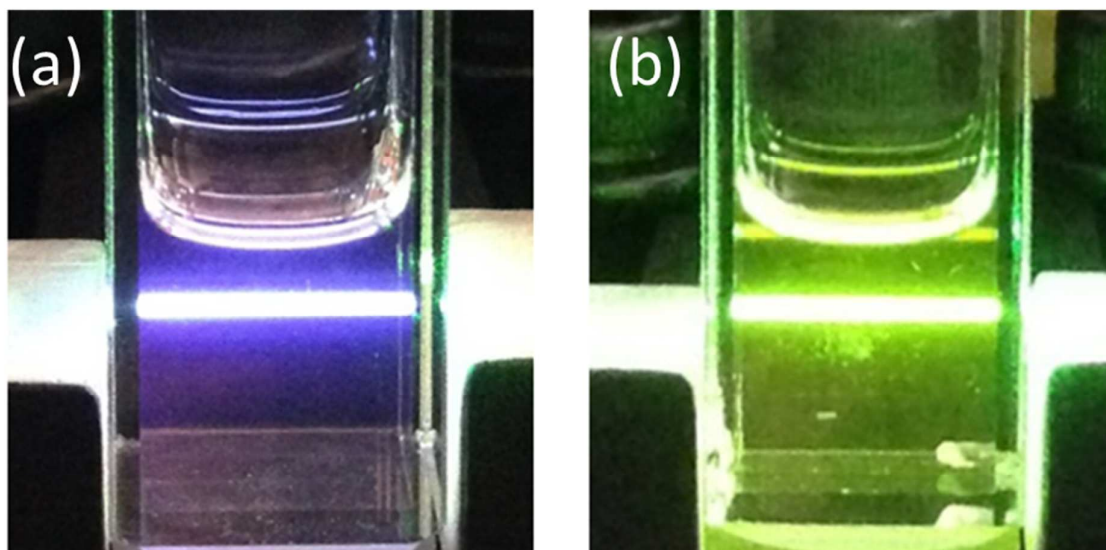

Figure S15. Photographs of upconversion in a cuvette containing (a) an optimized CdSe/9-ACA/DPA and (b) a CdSe/ODPA/DPA mixture (the spectra of these samples are shown in Figure S7). They were excited with a focused cw 532 nm laser. The violet DPA output in (a) swamps the the green beam that is clearly seen in (b), where no upconversion takes place. This indicates the enhancement of the upconverted fluoresecence by the 9-ACA ligand. The photographs were taken with an Iphone 5 and were not modified in any way.

9. References

(1) Carbone, L.; Nobile, C.; Giorgi, M. D.; Sala, F. D.; Morello, G.; Pompa, P.; Hytch, M.; Snoeck, E.; Fiore, A.; Franchini, I. R.; Nadasan, M.; Silvestre, A. F.; Chiodo, L.; Kudera, S.; Cingolani, R.; Krahne, R.; Manna, L., Synthesis and Micrometer-Scale Assembly of Colloidal CdSe/CdS Nanorods Prepared by a Seeded Growth Approach. *Nano Lett.* **2007,** *7*, 2942-2950

(2) Yu, W. W.; Qu, L. H.; Guo, W. Z.; Peng, X. G., Experimental determination of the extinction coefficient of CdTe, CdSe, and CdS nanocrystals. *Chemistry of Materials* **2003,** *15*, 2854-2860.

(3) Lechner, R. T.; Fritz-Popovski, G.; Yarema, M.; Heiss, W.; Hoell, A.; Schulli, T. U.; Primetzhofer, D.; Eibelhuber, M.; Paris, O., Crystal Phase Transitions in the Shell of PbS/CdS Core/Shell Nanocrystals Influences Photoluminescence Intensity. *Chem. Mater.* **2014,** *26*, 5914-5922.

(4) Moreels, I.; Lambert, K.; Smeets, D.; De Muynck, D.; Nollet, T.; Martins, J. C.; Vanhaecke, F.; Vantomme, A.; Delerue, C.; Allan, G.; Hens, Z., Size-Dependent Optical Properties of Colloidal PbS Quantum Dots. *Acs Nano* **2009,** *3*, 3023-3030.

(5) Moreels, I.; Lambert, K.; De Muynck, D.; Vanhaecke, F.; Poelman, D.; Martins, J. C.; Allan, G.; Hens, Z., Composition and size-dependent extinction coefficient of colloidal PbSe quantum dots. *Chemistry of Materials* **2007,** *19*, 6101-6106.

(6) Lakowicz, J. R., *Principles of Fluorescence Spectroscopy*. Third ed.; Springer New York, NY: 2006.

(7) Montalti, M. C., A.; Prodi, L., *Handbook of photochemistry*. CRC Press, Boca Raton, Fl: 2006.